

Radical Ions of Crownophanes Derived from Tetraphenylethene. Solution Structures and Ion-Pairing Phenomena

Frédérique Barbosa,[†] Vincent Péron,[‡] Georg Gescheidt,^{*,‡} and Alois Fürstner[§]

Institute of Organic Chemistry, Department of Chemistry, University of Basel, St.-Johanns-Ring 19, CH-4056 Basel, Institute of Physical Chemistry, Department of Chemistry, University of Basel, Klingelbergstrasse 80, CH-4056 Basel, and Max-Planck-Institut für Kohlenforschung, Kaiser Wilhelm-Platz 1, D-45470 Mülheim/Ruhr

Received May 13, 1998

Radical anions and radical cations of parent tetraphenylethene (**1**) and its cyclophane derivatives **2–8** were generated by chemical methods. These paramagnetic species were characterized by their ESR and simultaneously recorded optical spectra. The hyperfine coupling constants were substantiated by ENDOR and their signs by general TRIPLE spectroscopy. The structures of the radical ions were established with the help of quantum chemical calculations. The electron distribution in the phane radical ions is closely related to that found for $1^{\cdot-}/1^{\cdot+}$. In the radical anions no specific complexation of alkali-metal counterions, K^+ and Li^+ , by the crown-ether moieties could be observed. When the radical cations were generated by oxidation with Tl^{III} trifluoroacetate in 1,1,1,3,3,3-hexafluoropropanol, distinctly different ESR spectra were recorded as with the use of other oxidants. This observation is rationalized by the characteristic solvation properties of 1,1,1,3,3,3-hexafluoropropanol.

Introduction

Organic molecules consisting of numerous π centers often are efficient electron donors and acceptors. Therefore, such organic molecules have been regarded as constituents of, e.g., redox switches^{1–11} or of organic wires.^{12–17}

The oxidation and the reduction potentials are closely related to the orbital energies of the frontier orbitals. For a π system, the energy gap between the highest occupied and lowest unoccupied orbital (HOMO–LUMO gap) decreases when the number of sp^2 -hybridized centers is increased. Consequently extended π systems can readily accept and donate electrons. One of the early examples

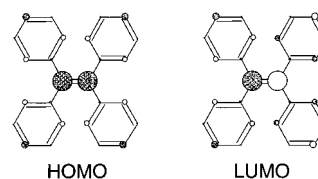
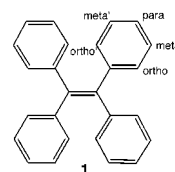


Figure 1. Frontier orbitals of **1** according to Hückel calculations.

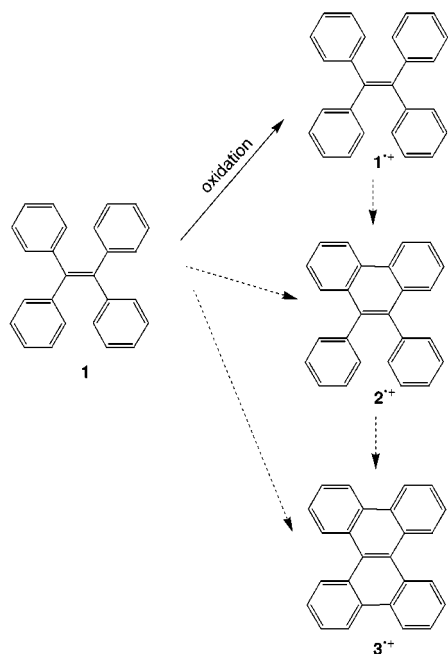
in this respect is tetraphenylethene (**1**) consisting of 26 conjugated π centers.



Both radical anions and radical cations of **1** generated by one-electron reduction and oxidation reactions have been analyzed in terms of their hyperfine data obtained from their ESR spectra.^{18–20} The proton-hyperfine coupling constants, a_H , of $1^{\cdot-}$ and $1^{\cdot+}$ indicate identical patterns due to the alternant connectivity of the π centers.²¹ The HOMO and the LUMO of **1** according to the Hückel model are shown in Figure 1.

In the oxidized and in the reduced stage, the central ethylene double bond is weakened because, for the radical cation, an electron is removed from an orbital with a strongly bonding interaction between the ethene C atoms, whereas for the radical anion, the interaction between

- [†] Institute of Organic Chemistry.
[‡] Institute of Physical Chemistry.
[§] Max-Planck-Institute für Kohlenforschung.
 (1) Daub, J.; Salbeck, J.; Knoechel, T.; Fischer, C.; Kunkely, H.; Rapp, K. M. *Angew. Chem.* **1989**, *101*, 1541.
 (2) Daub, J.; Fischer, C.; Salbeck, J.; Ulrich, K. *Adv. Mater.* **1990**, *2*, 366.
 (3) Daub, J.; Fischer, C.; Gierisch, S.; Sixt, J. *Mol. Cryst. Liq. Cryst. Sci. Technol., Sect. A* **1992**, *177*.
 (4) Daub, J.; Beck, M.; Knorr, A.; Spreitzer, H. *Pure Appl. Chem.* **1996**, *68*, 1399.
 (5) Achatz, J.; Fischer, C.; Salbeck, J.; Daub, J. *Chem. Commun.* **1991**, 504.
 (6) Bross, P. A.; Schoeberl, U.; Daub, J. *Adv. Mater.* **1991**, *3*, 198.
 (7) Knorr, A.; Daub, J. *Angew. Chem., Int. Ed. Engl.* **1995**, *34*, 2664.
 (8) Spreitzer, H.; Daub, J. *Liebigs Ann.* **1995**, 1637.
 (9) Scholz, M.; Gescheidt, G.; Schoeberl, U.; Daub, J. *Magn. Reson. Chem.* **1995**, *94*.
 (10) Tsigvoulis, G. M.; Lehn, J. M. *Adv. Mater.* **1997**, *9*, 39.
 (11) Tsigvoulis, G. M.; Lehn, J. M. *Adv. Mater.* **1997**, *9*, 627.
 (12) Baumgarten, M.; Muellen, K. *Top. Curr. Chem.* **1994**, *169*, 1.
 (13) Bohnen, A.; Koch, K. H.; Luettke, W.; Muellen, K. *Angew. Chem.* **1990**, *102*, 548.
 (14) Klaerner, G.; Mueller, M.; Morgenroth, F.; Wehmeier, M.; Soczka, G. T.; Muellen, K. *Synth. Met.* **1997**, *84*, 297.
 (15) Morgenroth, F.; Reuther, E.; Muellen, K. *Angew. Chem., Int. Ed. Engl.* **1997**, *36*, 631.
 (16) Mueller, M.; Morgenroth, F.; Scherf, U.; Soczka, G. T.; Klaerner, G.; Muellen, K. *Philos. Trans. R. Soc. London, Ser. A* **1997**, *355*, 715.
 (17) Quante, H.; Schlichting, P.; Rohr, U.; Geerts, Y.; Muellen, K. *Macromol. Chem. Phys.* **1996**, *197*, 4029.
 (18) Tabner, B. J. *J. Chem. Soc. A* **1969**, 2487.
 (19) Lundgren, B.; Levin, G.; Claesson, S.; Szwarc, M. *J. Am. Chem. Soc.* **1975**, *97*, 262.
 (20) Levin, G.; Claesson, S.; Szwarc, M. *J. Am. Chem. Soc.* **1972**, *94*, 8672.
 (21) Heilbronner, E.; Bock, H. *The HMO-Model and its Application*; Wiley and Verlag Chemie: London, New York, and Weinheim, 1976.

Scheme 1. Reactivity of $1^{\bullet+}$ According to Ref 25

these centers becomes antibonding. Therefore, isomerizations of tetraphenylethene-type molecules should occur preferably in these open-shell stages.

The geometrical consequences of an electron transfer to or from **1** were also inspected by electrochemical methods^{22,23} and electronic-absorption spectroscopy.²⁴

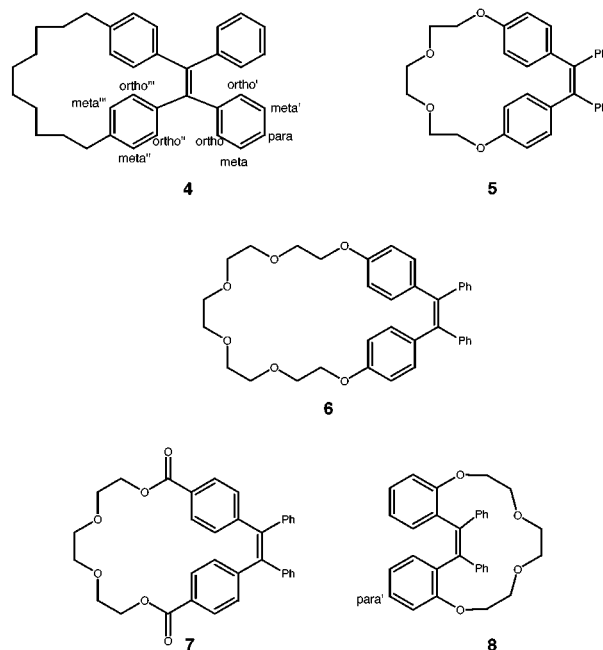
Five sets of hyperfine coupling constants, a_{H} , each due to four equivalent protons were reported for $1^{\bullet-}$ (0.209 mT (4 H, para), 0.167 mT (4 H, ortho), 0.136 mT (4 H, ortho'), 0.081 (4 H, meta), and 0.036 mT (4 H, meta')).¹⁸ These values are almost matched by those ascribed to $1^{\bullet+}$ (0.201, 0.150, 0.090, 0.083, and 0.050 mT, respectively).²⁵ This shows that the phenyl rings do not rotate freely on the hyperfine time scale and that the electron distribution in the radical anion and the radical cation are rather similar, in line with the pairing properties suggested by the Hückel model.

The conspicuous electron-accepting properties of **1** are indicated by the observation that the dianion 1^{2-} is formed at almost the same potential as the monoion²³ and often occurs as a byproduct when $1^{\bullet-}$ is generated by alkali-metal reductions of **1** in ethereal solvents. This is corroborated by the diminished ESR intensity of $1^{\bullet-}$ when the formation of tight ion pairs is promoted (high temperature, nonpolar solvents); the additional increase of the ESR line widths indicates the shorter lifetime of $1^{\bullet-}$ by a shift in the equilibrium $21^{\bullet-} \rightleftharpoons 1 + 1^{2-}$.

It has been shown that $1^{\bullet+}$ undergoes further reactions (Scheme 1).²⁵ Indeed the ESR spectrum attributable to the follow-up product dibenzophenanthrene $3^{\bullet+}$ grew into the ESR signal of $1^{\bullet+}$ with gradually increasing intensity (within ca. 0.5 h; this could also be followed by additional lines in the ENDOR spectrum). Presumably the formation of $3^{\bullet+}$ proceeds via 1,2-diphenyl derivative **2**.²⁵ The

mechanism leading to the occurrence of $3^{\bullet+}$, however, is unknown yet.

In this paper, we report on the generation of the radical anions and the radical cations of tetraphenylethene derivatives **4–8**. In these molecules two 1,2 phenyl groups are connected by a polymethylene (**4**) or polyoxyethylene (**5–8**) bridge either in the para (**4–7**) or in the ortho (**8**) positions.



The altered electronic structure, geometry, and the chelating ability of the oxygen atoms in the (crown)-phane moieties of **4–8** in respect to the parent compound **1** should lead to distinct changes of the geometry and the reactivity of the corresponding radical ions. The hitherto published a_{H} values of parent $1^{\bullet-}/1^{\bullet+}$ were only derived from the ESR spectra, and their signs were not yet determined experimentally; therefore, we have also reexamined these radical ions experimentally by the ENDOR and TRIPLE techniques²⁶ and by quantum chemical calculations.²⁷

Experimental Section

The radical anions of **1–8** were generated by dissolving the neutral compounds in 1,2-dimethoxyethane (DME) or tetrahydrofuran (THF) and reduced on a K mirror under high vacuum (10^{-5} Torr). The solvents were dried by refluxing over Na/K alloy for 4 days followed by distillation into a Schlenk tube containing Na/K alloy. After degassing, the solvents were stored under high vacuum (10^{-5} Torr).

The oxidation reactions were performed in CH_2Cl_2 (dried over molecular sieves under vacuum), trifluoroacetic acid (TFA), or 1,1,1,3,3,3-hexafluoropropan-2-ol (HFP) (all solvents highest available purity, Merck). Solutions of the oxidants (Ti^{III} trifluoroacetate, tris(*p*-bromophenyl)ammoniumyl hexachloroantimonate), and the parent compounds were mixed at low temperature (193 K) under vacuum (10^{-5} Torr). The reactors were transferred to the cavity of the ESR instrument, and the temperature was increased until an ESR signal occurred.

(22) Grzeszczuk, M.; Smith, D. E. *J. Electroanal. Chem. Interfacial Electrochem.* **1984**, *162*, 189.

(23) Shultz, D. A.; Fox, M. A. *J. Org. Chem.* **1990**, *55*, 1047.

(24) Suzuki, H.; Koyano, K.; Shida, T.; Kira, A. *Bull. Chem. Soc. Jpn.* **1979**, *52*, 2794.

(25) Ebersson, L.; Hartshorn, M. P.; Persson, O. *J. Chem. Soc., Perkin Trans. 2* **1995**, 1735.

(26) Kurreck, H.; Kirste, B.; Lubitz, W. *Electron Nuclear Double Resonance Spectroscopy of Radicals in Solution*; VCH: Weinheim, 1988.

(27) Batra, R.; Giese, B.; Spichy, M.; Gescheidt, G.; Houk, K. N. *J. Phys. Chem.* **1996**, *100*, 18371.

Table 1. Selected a_H of Radical Anions 1^- and 4^- – 8^- (All Given a_H Are Attributed to Two Equivalent Protons Except for 8^- (1H))

	T/K	a_H /mT (for the labeling of the positions, see the formulas)													
		meta	meta'	meta	meta'	ortho	ortho'	ortho	ortho'	ortho	ortho'	para			
1^- / K ⁺ / THF	273	+0.036	+0.081	+0.036	+0.081	-0.136	-0.167	-0.136	-0.167	-0.209					
4^- / K ⁺ / THF	193	+0.008	+0.022	+0.036	+0.080	-0.127	-0.146	-0.184	-0.184	-0.230	+0.252				
4^- / Li ⁺ / THF	273	+0.006	+0.037	+0.080	+0.096	-0.127	-0.149	-0.180	-0.180	-0.231	+0.251				
5^- / K ⁺ / THF	193	+0.006	+0.035	+0.035	+0.083	-0.105	-0.131	-0.161	-0.209	-0.267					
5^- / Li ⁺ / THF	193	+0.007	+0.035	+0.035	+0.084	-0.104	-0.131	-0.161	-0.209	-0.267					
6^- / K ⁺ / THF	193	+0.019	+0.036	+0.036	+0.084	-0.114	-0.142	-0.156	-0.198	-0.254					
6^- / Na ⁺ / THF	193	+0.018	+0.036	+0.036	+0.085	-0.117	-0.142	-0.156	-0.196	-0.250					
6^- / Li ⁺ / THF	193	+0.018	+0.037	+0.077	+0.086	-0.110	-0.137	-0.159	-0.203	-0.263					
7^- / K ⁺ / THF	193	-0.022	+0.042	+0.052	+0.068	-0.104	-0.124	-0.210	-0.229	-0.278					
8^- / K ⁺ / THF	193	+0.004	+0.028	+0.043	+0.061	+0.075	+0.094	-0.106	-0.122	-0.132	-0.170	-0.185	-0.204	0.217	0.239
8^- / Li ⁺ / THF	193	+0.022	+0.035	+0.046	+0.061	+0.081	+0.091	-0.111	-0.122	-0.134	-0.157	-0.185	-0.228	-0.242	-0.285

The electronic absorption spectra of the solutions containing the radical ions were taken inside the microwave cavity in the same region of the sample tube and simultaneously with the ESR spectra using a specially developed coupling of fiber optics to the cavity of the ESR spectrometer²⁸ and a J&M (Aalen, Germany) TIDAS diode array spectrometer (220–1021 nm).

ESR spectra were taken on a Varian E9 or Bruker ESP 300 spectrometer. The latter instrument was also used for ENDOR and general TRIPLE measurements.

The ESR spectral simulations were performed with the freeware program Winsim.²⁹

The Hückel MO calculations were done with the program MachMO.³⁰ The MOPAC 6.0 package³¹ was used for the semiempirical AM1³² and MNDO^{33,34} method whereas the ab initio and density functional theory (DFT) calculations were performed with Gaussian 94.³⁵

The syntheses of **4–8** were already reported.³⁶

Results and Discussion

Simultaneous in Situ Detected ESR and Optical Spectra of the Radical Anions. The radical anions of **1** and **4–8** were generated by reduction on a potassium mirror in THF, and their ESR spectra were studied between 193 and 273 K. In this temperature range, the ESR spectra remained almost unchanged and were only poorly resolved. The application of ENDOR spectroscopy reveals that the isotropic ¹H-hyperfine coupling constants, a_H , remain almost temperature invariable (Table 1). Addition of LiCl to the solutions of the radical anions generally did not lead to the detection of significantly different ESR/ENDOR spectra; only in the case of 6^- a slight increase of the biggest a_H was noted. Possibly, interaction of the crown ether moiety with Li⁺ leads to a small change of the twist of the phenyl groups without changing the overall C_s symmetry. The macrocycle 18-crown-6 is a favored ligand for the K⁺ cation. Thus,

ESR

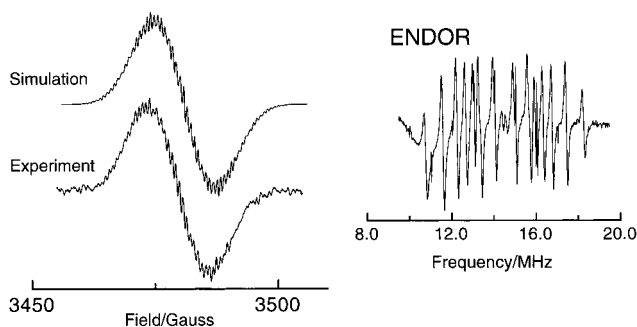


Figure 2. ESR (experimental and simulation) and ENDOR spectra of 4^- (solvent, THF; counterion, K⁺; temperature 243 K).

crownophane **6** should bind to K⁺ (and likewise Na⁺). Reduction of **6** in THF on a Na mirror led to the detection of the same a_H as with K⁺ as the counterion. Thus, no specific interaction between the crown-ether moiety and these alkali-metal cations could be established.

In agreement with formerly published data,¹⁸ our ENDOR spectra bear out that the parent radical anion 1^- possesses five sets of four equivalent protons. As expected, the free rotation of the four phenyl groups is restricted and the two ortho and the two meta positions are not equivalent. The biggest a_H (0.209 mT) is assigned to the para hydrogen whereas the a_H of 0.167 and 0.136 mT stem from the two different ortho protons. The smallest a_H of 0.081 and 0.036 mT consequently are attributed to the meta protons. A detailed assignment of the a_H can be achieved by comparing the experimental values with the calculated ones (see below).

The connection of the 1,2 diphenyl groups by an alkyl or polyoxyethylene bridge as in **4–8** diminishes the C_{2v} symmetry of the parent tetraphenylethene. In **4–8** the maximum achievable symmetry is C_s with pairwise equivalent phenyl groups. The decrease of symmetry depends on the conformation of the connecting chain. It is shown in Table 1 that 4^- – 7^- possess eight or nine different a_H . Moreover, the ESR simulations indicate that all a_H correspond to at least two equivalent protons (Figure 2) revealing that the phenyl groups are pairwise equivalent (C_s symmetry). In principle, the sizes of the a_H have a very similar pattern as those of parent 1^- . The positive sign of the biggest a_H of 4^- (0.252 mT) suggests that this a_H can be attributed to the β -methylene protons of the decamethylene chain. Accordingly the a_H of 0.235 mT is assigned to the para protons of the unsubstituted phenyl groups. The remaining a_H then belong to the ortho (negative sign) and meta (positive sign) positions

(28) Gescheidt, G. *Rev. Sci. Instr.* **1994**, *65*, 2145.

(29) Duling, D. R. *PEST Winsim*; NIEHS, Research Triangle Park, NC, 1995.

(30) Huber, H. *MachMO*; University of Basel, Basel, 1985.

(31) Seiler, F. J. *MOPAC 6.0*; Res. Lab., U. S. Air Force Academy, Colorado Springs, 1994.

(32) Dewar, M. J. S.; Zoebisch, E. G.; Healy, E. F.; Stewart, J. J. P. *J. Am. Chem. Soc.* **1985**, *107*, 3902.

(33) Thiel, W. *QCPE No. 438*; QCPE, Bloomington, IN, 1982.

(34) Dewar, M. J. S. *J. Am. Chem. Soc.* **1977**, *99*, 4899.

(35) Frisch, M. J.; Trucks, G. W.; Schlegel, H. B.; Gill, P. M. W.; Johnson, B. G.; Robb, M. A.; Cheeseman, J. R.; Keith, T.; Petersson, G. A.; Montgomery, J. A.; Raghavachari, K.; Al-Laham, M. A.; Zakrzewski, V. G.; Ortiz, J. V.; Foresman, J. B.; Peng, C. Y.; Ayala, P. Y.; Chen, W.; Wong, M. W.; Andres, J. L.; Replogle, E. S.; Gomperts, R.; Martin, R. L.; Fox, D. J.; Binkley, J. S.; Defrees, D. J.; Baker, J.; Stewart, J. P.; Head-Gordon, M.; Gonzalez, C.; Pople, J. A. *Gaussian 94, Revision B.2*; Gaussian, Inc.: Pittsburgh, PA, 1995.

(36) Fuerstner, A.; Seidel, G.; Kopiske, C.; Krueger, C.; Mynott, R. *Liebigs Ann.* **1996**, *5*, 655.

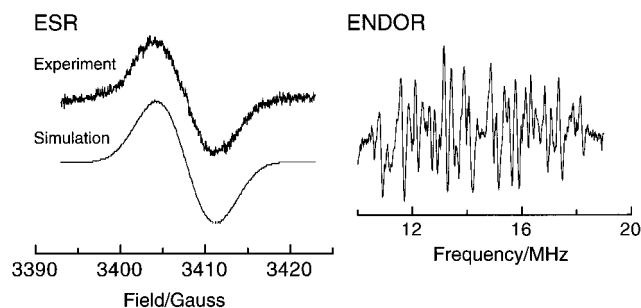


Figure 3. ESR (experimental and simulation) and ENDOR spectra of $8^{\bullet+}$ (solvent, DME; counterion, K^+ ; temperature 193 K).

(Table 1). In $5^{\bullet-}$ – $7^{\bullet-}$ the highest a_H have a negative sign and in analogy to $1^{\bullet-}$ belong to the para protons of the 1,2 phenyl groups. The remaining a_H correspond to those of $4^{\bullet-}$ and are assigned in an analogous way.

The number of a_H detected in the ENDOR spectra of $8^{\bullet-}$ is 14 vs 8 or 9 in the remaining crownphanes (Figure 3, right), and the simulation of the ESR spectrum is successfully achieved when each of these coupling constants is attributed to one single proton (Figure 3). This exhibits that bridging at the ortho positions of **8** causes a rigid arrangement of the 1,2-phenyl groups; i.e., the free rotation of these phenyl groups is hindered and a lowering of the symmetry arises (on the time scale of the ESR experiment).

It is noteworthy that the a_H of the radical anions and their multiplicities are almost independent of the temperature and the counterion. No significant changes can be detected on going from the relatively huge and polarizable counterion K^+ to the hard and small Li^+ (Table 1). Comparison of the a_H of $4^{\bullet-}$ containing a decamethylene bridge with $5^{\bullet-}$ in which the 10-center bridge contains four oxygen atoms reveals only marginal differences caused by two additional a_H in $4^{\bullet-}$ stemming from two β -protons of the decamethylene group and some deviations in the a_H values which can be traced back to differing electronic effects of the CH_2 groups and O atoms. It seems justified to assume that the Coulombic interaction between the negatively charged tetraphenylethene π system and the alkali-metal cation dominates the complexation at the crownophane moiety. Even in the case of **7** where the para benzo ester group leads to a concentration of the negative charge at the carbonyl O atoms, no particular ion-pairing effects by the Li^+ cation can be established.

The electronic absorption spectra of $1^{\bullet-}$ and $4^{\bullet-}$ – $8^{\bullet-}$ show comparable patterns with prominent bands at ca. 500 nm and 600–800 nm (Figure 4) and agree well with the spectra of $1^{\bullet-}$ published previously.^{19,24} Even in the case of $7^{\bullet-}$ at which a Li^+ cation could also bind to the carbonyl oxygen, addition of LiCl does not affect the electronic spectrum (see insert in Figure 4). The band at 600–800 nm is assigned to the SOMO–LUMO + 1 transition.

Simultaneous in Situ Detected ESR and Optical Spectra of the Radical Cations. The radical cation of **1** was described many years before by Lewis and Singer³⁷ and more recently by Ebersson and co-workers.²⁵ Our ESR spectra obtained after chemical oxidation of **1** by various methods and ascribed to $1^{\bullet+}$ correspond to the

experimental spectra already reported. The use of the ENDOR technique reveals, in agreement with Ebersson's data, that five different a_H values, each belonging to four equivalent protons, lead to the observed line pattern. This corroborates the finding that the pairs of ortho and meta protons in $1^{\bullet+}$ are not equivalent in the temperature range from 193 to 273 K.

Oxidation of **4**–**8** with Tl^{III} trifluoroacetate or tris(*p*-bromophenyl)ammoniumyl hexachloroantimonate in HFP, trifluoroacetic acid, or CH_2Cl_2 as the solvent led to the detection of ESR spectra. In most cases the ESR signals are attributable to the radical cations of **4**–**8** but often also represent superimposed signals.

When crownophane **5** is oxidized with Tl^{III} trifluoroacetate in CH_2Cl_2 a partly resolved ESR spectrum is detected. The simulation of the ESR curve with the coupling constants taken from the corresponding ENDOR spectrum leads to a favorable agreement when each a_H is attributed to two equivalent protons (Figure 5).

Oxidation of **4** with Tl^{III} trifluoroacetate in CH_2Cl_2 , at 193 K leads to an ESR spectrum with a large positive a_H of +0.493 mT (2 H), marking a slow-exchange between the two β -methylene protons on the hyperfine time scale. At 273 K this coupling is replaced by $a_H = 0.292$ mT (fast exchange, four equivalent protons). Owing to the unresolved ESR signal, a specific simulation of the dynamic process of the conformational interconversion of the decamethylene chain is not practicable. The free enthalpy of the interconversion can be estimated to ca. 25 $kJ \cdot mol^{-1}$ based on the difference of the coupling constants in the slow-exchange time domain and the temperature at which the equilibration of the two a_H values occurs.³⁸ The a_H of $5^{\bullet+}$ and $6^{\bullet+}$ represented by the ENDOR spectrum are rather similar to those of $4^{\bullet+}$ except that the a_H of the β -protons are missing because the *p*-methylene group is replaced by O atoms (Table 2). The carbonyl groups in **7** with their electron-accepting effect shift the positive charge and the spin to the two unsubstituted phenyl groups. Therefore the a_H attributed to the para protons increase relative to $1^{\bullet+}$ and $4^{\bullet+}$ – $6^{\bullet+}$. In $8^{\bullet+}$ where the $-O((CH_2)_2O)_2(CH_2)_2O-$ bridge is attached at the ortho positions where the MO coefficients are smaller than in the para positions, the a_H become close to those of parent $1^{\bullet+}$ (Table 2).

Generally, the ESR spectra ascribed to the radical cations of **4**–**8** generated by oxidation with Tl^{III} trifluoroacetate in CH_2Cl_2 or tris(*p*-bromophenyl)ammoniumyl hexachloroantimonate can be simulated using the a_H and assuming pairwise equivalent protons. Therefore it seems justified that the maximum achievable C_2 symmetry of $4^{\bullet+}$ – $8^{\bullet+}$ exists on the hyperfine time-scale, i.e., the bridging in the para or ortho positions does not severely affect the symmetry of the electron distribution in the tetraphenylethene π system.

The solutions of $1^{\bullet+}$ and $4^{\bullet+}$ – $8^{\bullet+}$ in CH_2Cl_2 give rise to almost matching absorption spectra (Figure 6). As for the radical anions they agree very well to the spectra reported by Suzuki et al.²⁴ Two main bands are located at ca. 500 and ca. 880 nm and a third band around 630 nm is discernible. According to PPP calculations the absorption at ca. 500 nm was assigned to the SOMO–LUMO transition whereas long wave band was ascribed to a SOMO–1–SOMO transition. It is noteworthy that

(37) Lewis, I. C.; Singer, L. S. *J. Chem. Phys.* **1965**, *43*, 2712.

(38) Friebolin, H. *Basic One- and Two-Dimensional NMR Spectroscopy*, 2nd ed.; VCH: Weinheim, 1993.

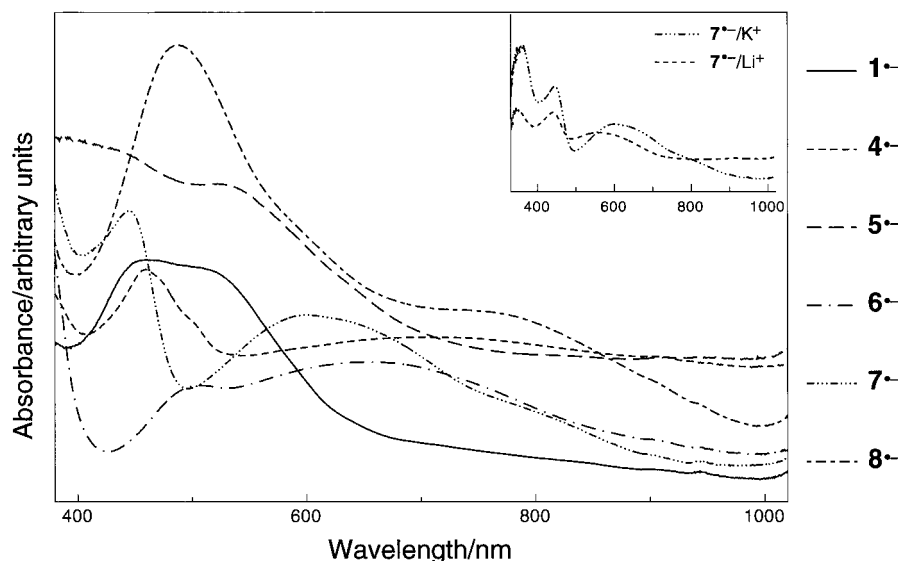


Figure 4. Electronic absorption spectra of $1^{\bullet+}$ and $4^{\bullet+}$ – $8^{\bullet+}$ measured simultaneously with the ESR spectra (solvent, THF; counterion, K^+ ; temperature 243 K).

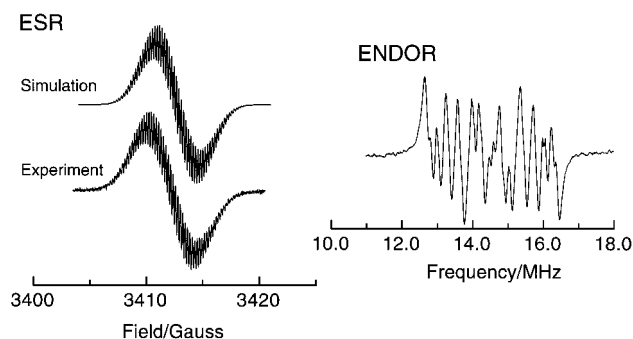


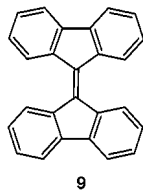
Figure 5. ESR (experimental and simulation) and ENDOR spectra of $5^{\bullet+}$ (solvent, CH_2Cl_2 ; counterion, CF_3COO^- ; temperature 273 K).

the spectra are almost identical for all radical cations and correspond to those of $1^{\bullet+}$ generated by γ irradiation in a Freon matrix.²⁴

Effect of HFP as the Solvent. It is peculiar that the use of HFP as solvent leads to markedly altered ESR and ENDOR spectra particularly for $4^{\bullet+}$ – $6^{\bullet+}$ and $8^{\bullet+}$ but not for the ester $7^{\bullet+}$. As an example, the ESR spectra recorded after oxidation of $7^{\bullet+}$ is shown in Figure 7.

The prominent differences between the spectra obtained after Tl^{III} trifluoroacetate oxidation in CH_2Cl_2 and in HFP as the solvent are: (i) In HFP a higher number of coupling constants is detected. (ii) The a_H measured in HFP reach significantly higher values than in CH_2Cl_2 .

A rationale for these observations could be the intramolecular coupling reaction analogous to $1^{\bullet+}$ shown in Scheme 1.²⁵ But none of the a_H detected are consistent with rearrangement products such as radical cations derived from dibenzoterphenyl (**3**) or 9,9'-bifluorene (**9**).



More likely, the experimental data point to a perturbed

geometry of the radical cations of $5^{\bullet+}$ – $8^{\bullet+}$ in which the spin is unevenly distributed between the four benzene rings. Such a distortion can be caused by an altered (rigid) arrangement of the polyoxyethylene chains induced by the binding of a cation to the crown ether moiety. Obviously, with the use of $Tl(III)$ trifluoroacetate Tl^{3+} cations are present in the solutions containing the radical cations. It is known that HFP preferentially solvates anions. If the trifluoroacetate anions are solvated by HFP, "naked" Tl^{3+} ions remain in solution and can bind to the crown-ether moieties of $5^{\bullet+}$ – $8^{\bullet+}$. The interaction of the radical cation with Tl^{3+} leads to four positive charges within the molecular assembly. However, the Coulombic repulsion between the delocalized π radical cation and Tl^{3+} embedded in the crown ether moiety is weak because of the remote sites carrying the positive charges.

To test whether Tl^{3+} cations, in the presence of CF_3COO^- bind to crown ethers in HFP, we recorded NMR spectra of solutions of 12-crown-4 and 15-crown-5 in HFP and in CH_2Cl_2 both in the presence and in the absence of $Tl(III)$ trifluoroacetate. The conspicuous observation was that line broadening of the signal attributed to the crown ether protons occurred only when HFP was the solvent and the $Tl(III)$ salt was present. Therefore it seems justified to assume that Tl^{3+} interacts with the polyoxymethylene bridges in $5^{\bullet+}$ – $8^{\bullet+}$. It is also likely that this effect is preferably manifested by the ESR technique because of its faster dynamic time scale compared to NMR. A more detailed and extended study is, however, necessary to rigorously establish these assumptions.

Calculations

The method of choice for the calculation of a_H in radical ions of extended (planar) π systems has been the Hückel model.^{21,39} Indeed, application of this simplistic procedure in these particular cases leads to a pertinent agreement of the experimental and the calculated values. A prerequisite is the use of empirical perturbation parameters which mimic the geometrical and the elec-

(39) Gerson, F. *Hochauflösende ESR-Spektroskopie*; Verlag Chemie: Weinheim, 1967.

Table 2. Selected a_H of Radical Cations $1^{+\cdot}$ and $4^{-\cdot}-8^{+\cdot}$ (All Given a_H Are Attributed to Two Equivalent Protons Except for $8^{+\cdot}$ (IH) and the ESR Spectra Taken in HFP as the Solvent)

	oxidant/solvent	T/K	a_H/mT														
			+0.050	+0.087	-0.139	-0.152	-0.209	-0.131	-0.146	-0.156	-0.175	+0.493	-0.134	-0.147	+0.156	-0.166	+0.300
$1^{+\cdot}$	Tl(O ₂ CCF ₃) ₃ /CH ₂ Cl ₂	193	+0.006	+0.044	+0.071	+0.084	-0.122	-0.131	-0.146	-0.156	-0.175	+0.493	-0.134	-0.147	+0.156	-0.166	+0.300
$4^{+\cdot}$	Tl(O ₂ CCF ₃) ₃ /CH ₂ Cl ₂	193	+0.006	+0.044	+0.065	+0.083	-0.123	-0.130	-0.145	-0.155	-0.170	+0.292 (4 H)	-0.133				
	Tl(O ₂ CCF ₃) ₃ /HFP	303	+0.006	+0.020	+0.032	+0.044	+0.056	+0.067	+0.082	+0.088	-0.111	-0.118	-0.140				
$5^{+\cdot}$	Tl(O ₂ CCF ₃) ₃ /CH ₂ Cl ₂	193	+0.006	+0.021	+0.024	+0.032	+0.063	+0.067	-0.083	-0.089	-0.104	-0.120	-0.140				
	(p-Br-C ₆ H ₄) ₃ N ⁺ • SbCl ₆ ⁻ /HFP	273	+0.004	+0.013	+0.020	+0.030	+0.061	+0.071	-0.095	-0.101	-0.123	-0.129	+0.228				
	Tl(O ₂ CCF ₃) ₃ /HFP	273	+0.003	+0.009	-0.020	+0.035	+0.054	+0.069	-0.083	+0.124	-0.165	-0.198	+0.315				
$6^{+\cdot}$	Tl(O ₂ CCF ₃) ₃ /CH ₂ Cl ₂	273	+0.006	+0.017	+0.028	+0.042	+0.069	-0.095	-0.119	-0.137	-0.147	-0.163					
	Tl(O ₂ CCF ₃) ₃ /HFP	273	-0.022	-0.083	+0.125	-0.178	+0.196	+0.231	+0.315								
$7^{+\cdot}$	Tl(O ₂ CCF ₃) ₃ /CH ₂ Cl ₂	193	+0.012	+0.049	+0.080	+0.080	+0.089	-0.125	-0.137	-0.150	-0.165	-0.249					
	Tl(O ₂ CCF ₃) ₃ /HFP	273	+0.011	+0.045	+0.064	+0.080	+0.090	-0.123	-0.160	-0.160	-0.173	-0.269					
$8^{+\cdot}$	Tl(O ₂ CCF ₃) ₃ /CH ₂ Cl ₂	193	+0.051	+0.080	+0.107	+0.080	+0.090	-0.123	-0.160	-0.115	-0.147	-0.189					
	Tl(O ₂ CCF ₃) ₃ /HFP	273	+0.007	+0.020	+0.043	+0.050	+0.063	+0.082	+0.093	-0.105	-0.116	-0.119	-0.143	-0.157	-0.193	-0.207	

tronic influences of the alkylidene or polyoxyethylene bridges. The steric congestion between the facing ortho H atoms is accounted by $k_{ortho} = -0.1\beta$, the inductive effect of the alkyl or O-alkyl groups by $k = -0.3$, and the O atoms in the carbonyl groups of extended π system of **7** by $k_O = 2.0$ and $h_{CO} = 1.56\beta$.

In the recent time it was shown that density functional theory (DFT)^{40,41} is a favorable tool for the calculation of isotropic hyperfine coupling constants in a variety of radicals (see, e.g. ref 27 and 42–48). In view of the considerable size of compounds **5–8**, we have first inspected if it is necessary to optimize the geometry of the entire molecules or if it is sufficient to regard only the π system in which the spin and the charge are delocalized in the radical ions. Molecular models indicate that the polyoxyethylene and the polymethylene chains connecting the two phenyl groups possess numerous minimum-energy conformations and allow an almost unrestricted rotation of the phenyl groups (except **8**). Optimizations (UHF/3-21G*) of $7^{-\cdot}$ and $7^{+\cdot}$ show that the tetraphenylethene fragment adopts an almost matching geometry as if the crown ether moiety was replaced by a COOH substituent. Therefore we have replaced the chains by OCH₃ (**5**, **6**, **8**) and COOH (**7**) groups to reduce the CPU times. On the basis of the minimized geometry, single-point calculations with the B3LYP^{49,50} hybrid functional were performed. Roughly, the a_H calculated by these procedures correspond to the shapes of the Hückel frontier orbitals; however, the agreement between the theoretical and the experimental data is best for the ab initio/DFT combination.²⁷ The data are compared in Figures 8 and 9 for the radical anions and cations, respectively, of parent **1**. Analogous correlations also hold for **5/6**, **7**, and **8**. This is shown in Tables 3 and 4 for the radical anions and radical cations, respectively. Para'', para''' di(methoxy) substituted **1** served as model for **5/6** whereas for **7** both the parent compound and the model with para'', para''' di(COOH) was compared. Moreover, Table 3 contains calculations of three ion pairs of **7** (MNDO geometry optimization, see below). The geometry was optimized with AM1 or UHF/3-21G* whereas the single-point calculations were performed with the UB3LYP/6-31G*. Both protocols point to comparable shapes of the singly occupied orbitals. Typically, the UHF/3-21G* geometry leads to a better agreement of experimental and calculated data than AM1.

Geometry of the Radical Ions

The geometry of the radical ions of tetraphenylethene has already been subject of investigations. On the basis

(40) Kohn, W.; Becke, A. D.; Parr, A. G. *J. Phys. Chem.* **1996**, *100*, 12974.

(41) Parr, R. G.; Yang, W. *Density Functional Theory of Atoms and Molecules*; Oxford University Press: Oxford, 1989.

(42) Adamo, C.; Barone, V.; Fortunelli, A. *J. Phys. Chem.* **1994**, *98*, 8648.

(43) Barone, V. *Theor. Chim. Acta* **1995**, *3*, 113.

(44) Eriksson, L. A.; Malkin, V. G.; Malkina, O. L.; Salahub, D. R. *J. Chem. Phys.* **1993**, *99*, 9756.

(45) Eriksson, L. A.; Malkina, O. L.; Malkin, V. G.; Salahub, D. R. *J. Chem. Phys.* **1994**, *100*, 5066.

(46) Himio, F.; Eriksson, L. A. *J. Chem. Soc., Faraday Trans.* **1995**, *91*, 4343.

(47) Malkin, V. G.; Malkina, O. L.; Eriksson, L. A.; Salahub, D. R. In *Theoretical and Computational Chemistry*; Seminario, J. M., Politzer, P., Eds.; Elsevier: Amsterdam, 1995; Vol. 2.

(48) Gano, J. E.; Jacob, E. J.; Sekher, P.; Subramaniam, G.; Eriksson, L. A.; Lenoir, D. *J. Org. Chem.* **1996**, *61*, 6739.

(49) Becke, A. D. *Phys. Rev. A* **1988**, *38*, 3098.

(50) Becke, A. D. *J. Chem. Phys.* **1993**, *98*, 1372.

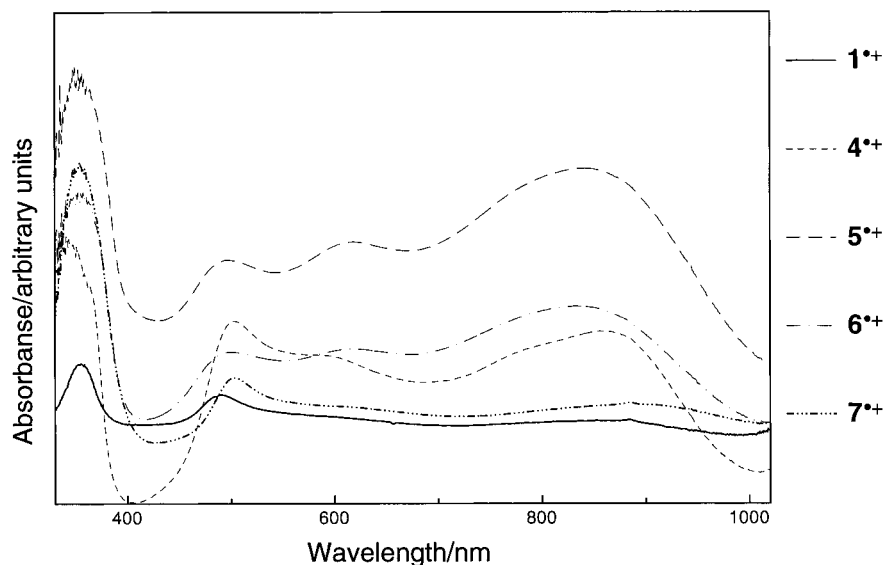


Figure 6. Electronic absorption spectra of $1^{\bullet+}$ and $4^{\bullet+}$ – $7^{\bullet+}$ measured simultaneously with the ESR spectra (solvent, CH_2Cl_2 ; counterion, SbCl_6^- ; temperature 263 K).

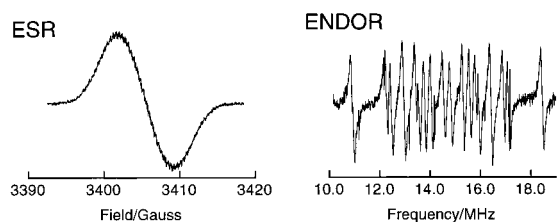


Figure 7. ESR and ENDOR spectra of $7^{\bullet+}$ (solvent, HFP; counterion, CF_3COO^- ; temperature 273 K).

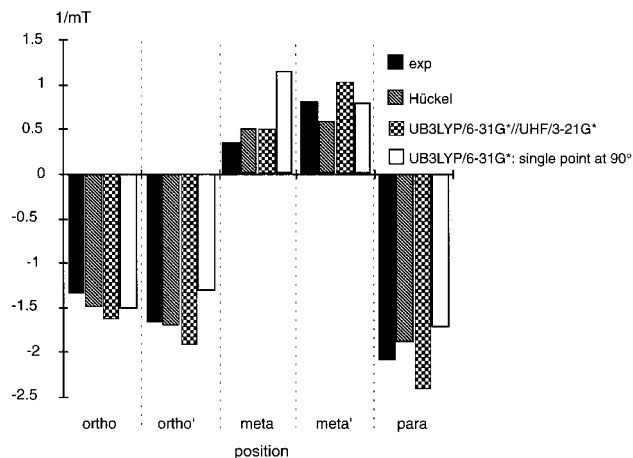


Figure 8. Comparison of experimental and calculated a_{H} of $1^{\bullet-}$.

of the optical spectroscopy, it was postulated that $1^{\bullet-}$ has a different geometry than $1^{\bullet+}$. Whereas in the radical anion the central bond is reported to be twisted by a considerable amount (up to almost 90°), it was assumed to be almost unaffected in the radical cation.²⁴ On the other hand, electrochemical studies indicated that the twist around the central bond is much less pronounced ($\leq 30^\circ$) and that phenyl-ring torsion plays an important role for the geometry (and ion-pairing properties) of $1^{\bullet-}$.²³

In this respect it is interesting to compare the geometry calculated for the neutral **1**, its radical anion, and the radical cation. In agreement to π electron models the ethenic bond of tetraphenylethene (**1**) is weakened upon

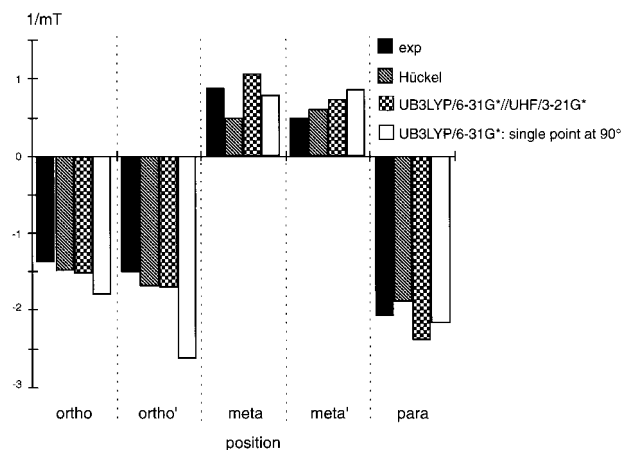


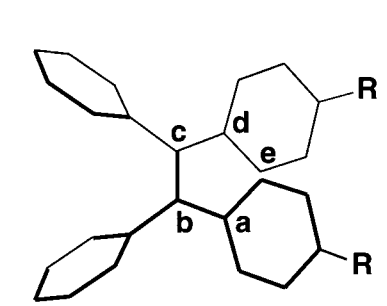
Figure 9. Comparison of experimental and calculated a_{H} of $1^{\bullet+}$.

electron removal or electron addition (Figure 10). As a consequence, a twist of this bond is predicted by the AM1 model and the ab initio procedure for both radical ions. The twist angle is rather similar in both radical ions not exceeding 38° . For both methods, this angle is 4 – 8° larger for the radical anion. Compared with the X-ray structures of neutral crownphanes in which the corresponding twist amounts to 8 – 14° ³⁶ the electron-transfer induces an additional bending of 20 – 30° (Figure 10).

The phenyl groups are twisted out of the ethylenic plane only by ca. 33° in $1^{\bullet-}$ and $1^{\bullet+}$. For the neutral crownphanes **5**–**7**, these angles amount to about 50° according to the X-ray-determined geometry.³⁶

The good agreement between the experimental and the calculated a_{H} suggests that the geometry of the radical ions of **1** and phanes **4**–**8** is very similar. This is also borne out by AM1 and Hartree–Fock optimizations of the radical cation and anion of **7** and **8** and model system of **5/6**, and **7** in which the twist angles of the ethenic bond and the phenyl groups reach almost the same values as in $1^{\bullet-}/1^{\bullet+}$ (Figure 10).

To test the significance of these statements we have twisted the central bond in the optimized geometry of $1^{\bullet-}/1^{\bullet+}$ by 90° and computed the a_{H} by the unrestricted



	Method	b—c/Å	∠abcd/°	∠bcde
1	UHF/3-21G*	1.335	6.9	54.4
1 ^{•-}	AM1	1.415	34.3	31.3
1 ^{•-}	UHF/3-21G*	1.430	38.0	31.9
1 ^{•+}	AM1	1.429	33.4	32.7
1 ^{•+}	UHF/3-21G*	1.419	26.1	38.8
model of 5/6 ^{•-}	AM1	1.415	34.2	31.7
model of 5/6 ^{•-}	UHF/3-21G*	1.431	37.9	30.4
model of 5/6 ^{•+}	AM1	1.429	33.6	35.6
model of 5/6 ^{•+}	UHF/3-21G*	1.421	27.6	40.1
model of 7 ^{•-}	AM1	1.415	33.2	37.9
model of 7 ^{•-}	UHF/3-21G*	1.430	37.3	38.1
model of 7 ^{•+}	AM1	1.428	33.2	30.4
model of 7 ^{•+}	UHF/3-21G*	1.418	25.9	37.8
7 ^{•-}	UHF/3-21G*	1.434	37.7	37.9
7 ^{•+}	UHF/3-21G*	1.419	26.2	36.2
8 ^{•-}	AM1	1.412	35.4	33.4
8 ^{•-}	UHF/3-21G*	1.427	33.9	32.1
8 ^{•+}	AM1	1.434	35.6	34.4
8 ^{•+}	UHF/3-21G*	1.424	30.4	40.3

for model of 5/6: R = -OCH₃
for model of 7: R = -COOH

Figure 10. Selected geometry parameters of tetraphenylethene and phane radical cations and radical anions according to quantum mechanical calculations.

Table 3. Calculated a_{H} of the Aromatic Protons of the Radical Anions of 1, 7, and 8, Model Systems of 5–7, and Ion Pairs of 7^{•-}/Li⁺ (for model systems of 5/6, see Figure 10)

method	a_{H} /mT (for the labeling of the positions, see the formulas)									
	meta	meta'	meta''	meta'''	ortho	ortho'	ortho''	ortho'''	para	para'
1 ^{•-}	UB3LYP/6-31G**/UHF/3-21G*	+0.051	+0.102	+0.051	+0.102	-0.164	-0.192	-0.192	-0.164	-0.242
1 ^{•-}	UB3LYP/6-31G**/AM1	+0.078	+0.123	+0.078	+0.123	-0.184	-0.227	-0.227	-0.184	-0.272
1 ^{•-} 90°	UB3LYP/6-31G* (SinglePoint)	+0.114	+0.079	+0.114	+0.079	-0.153	-0.131	-0.131	-0.153	-0.173
model of [5/6] ^{•-}	UB3LYP/6-31G**/UHF/3-21G*	+0.068	+0.105	+0.065	+0.104	-0.183	-0.208	-0.144	-0.202	-0.275
model of [5/6] ^{•-}	UB3LYP/6-31G**/AM1	+0.083	+0.124	+0.094	+0.137	-0.195	-0.231	-0.176	-0.266	-0.283
7 ^{•-}	UB3LYP/6-31G**/UHF/3-21G*	+0.050	+0.084	+0.105	+0.065	-0.121	-0.137	-0.136	-0.162	-0.160
7 ^{•-}	UB3LYP/6-31G**/MNDO	+0.053	+0.089	+0.072	+0.092	-0.133	-0.114	-0.209	-0.188	-0.147
model of 7 ^{•-}	UB3LYP/6-31G**/UHF/3-21G*	+0.054	+0.088	+0.008	+0.052	-0.119	-0.132	-0.139	-0.167	-0.156
model of 7 ^{•-}	UB3LYP/6-31G**/AM1	-0.052	+0.088	+0.024	+0.081	-0.115	-0.137	-0.165	-0.206	-0.152
7 ^{•-} /Li ⁺ (A)	UB3LYP/6-31G**/MNDO	+0.006	+0.006	-0.144	-0.130	+0.005	+0.006	+0.061	+0.073	-0.003
7 ^{•-} /Li ⁺ (B)	UB3LYP/6-31G**/MNDO	-0.043	-0.041	+0.009	+0.006	+0.009	-0.011	+0.010	+0.008	-0.456
7 ^{•-} /Li ⁺ (C)	UB3LYP/6-31G**/MNDO	+0.084	+0.134	+0.106	+0.069	-0.193	-0.184	-0.098	-0.131	-0.201
8 ^{•-}	UB3LYP/6-31G**/UHF/3-21G*	+0.076	+0.111	+0.059	+0.056	-0.228	-0.257		-0.333	-0.101
8 ^{•-}	UB3LYP/6-31G**/AM1	+0.100	+0.141	+0.081	+0.077	-0.234	-0.264		-0.311	-0.123

Table 4. Calculated a_{H} of the Aromatic Protons of the Radical Cations of 1, 7, and 8 and Model Systems of 5–7 (for model systems of 5/6, See Figure 10)

method	a_{H} /mT (for the labeling of the positions, see the formulas)									
	meta	meta'	meta''	meta'''	ortho	ortho'	ortho''	ortho'''	para	para'
1 ^{•+}	UB3LYP/6-31G**/UHF/3-21G*	+0.106	+0.073	+0.106	+0.073	-0.153	-0.171	-0.171	-0.153	-0.239
1 ^{•+}	UB3LYP/6-31G**/AM1	+0.130	+0.092	+0.130	+0.092	-0.182	-0.201	-0.201	-0.182	-0.254
1 ^{•+} 90°	UB3LYP/6-31G* (SP)	+0.079	+0.085	+0.079	+0.085	-0.182	-0.264	-0.264	-0.182	-0.218
model of [5/6] ^{•+}	UB3LYP/6-31G**/UHF/3-21G*	+0.098	+0.058	+0.036	+0.027	-0.130	-0.137	-0.115	-0.163	-0.173
model of [5/6] ^{•+}	UB3LYP/6-31G**/AM1	+0.110	+0.067	+0.056	+0.047	-0.144	-0.154	-0.137	-0.193	-0.182
7 ^{•+}	UB3LYP/6-31G**/UHF/3-21G*	+0.099	+0.075	+0.119	+0.079	-0.156	-0.176	-0.151	-0.169	-0.251
model of 7 ^{•+}	UB3LYP/6-31G**/UHF/3-21G*	+0.101	+0.076	+0.119	+0.079	-0.157	-0.178	-0.142	-0.168	-0.258
model of 7 ^{•+}	UB3LYP/6-31G**/AM1	-0.118	+0.097	+0.122	+0.075	-0.184	-0.217	-0.143	-0.167	-0.289
8 ^{•+}	UB3LYP/6-31G**/UHF/3-21G*	+0.114	+0.086	+0.066	+0.054	-0.190	-0.260		-0.333	-0.142
8 ^{•+}	UB3LYP/6-31G**/AM1	+0.111	+0.084	+0.077	-0.115	-0.197	-0.213		-0.265	-0.007

B3LYP method. The thus-calculated a_{H} possess the same order of magnitude as the values obtained from the minimized geometry (Figures 8 and 9). It is, however, apparent that the a_{H} obtained from the optimized geometry represent a preferable agreement with the experimental values. In addition, we began optimizations with the diphenylmethylene fragments being orthogonal for both radical ions. In each case no minimum could be localized for an almost orthogonal arrangement of the two diphenylmethylene moieties.

Hence, we conclude that the bond lengths and angles indicated in Figure 10 represent relevant geometrical

parameters of the radical anions and cations derived from tetraphenylethene.

Ion Pairing in the Radical Anions. It is well established that the π system of 1^{•-} and its derivatives strongly interacts with its counterions.^{19,20,23,51} Therefore, it was of interest in how far the interaction of the (crown)ophane moiety affects the electron distribution in 4^{•-}–8^{•-}. No particular interactions between the alkylidene chain in 4 is expected whereas 5 and 7 (and with

(51) Cserhegyi, A.; Jagur, G. J.; Szwarc, M. *J. Am. Chem. Soc.* **1969**, *91*, 1892.

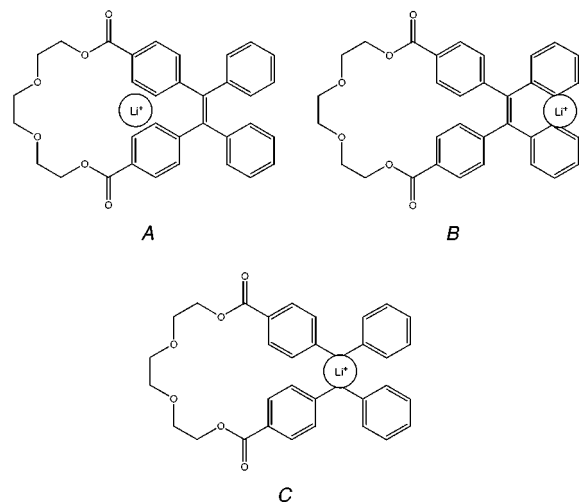


Figure 11. Ion-pair structures A, B, and C of $7^{\bullet-}/\text{Li}^+$.

some limitations **8**) with their 12-crown-4 type chain could serve as specific ligands for Li^+ and **6**, resembling 18-crown-6, could be specific for K^+ . Unexpectedly, the ESR data of the phane radical anions indicate no significant alternations with Li^+ , Na^+ , or K^+ as the counterion. All ESR spectra remained temperature invariable in the range from 193 to 273 K. As stated above, the differences in the a_{H} and their multiplicities can be traced back to the reduced symmetry of thephanes **4–8** in respect to parent **1** and to electronic effects of the alkyl, alkoxy, and acyl substituents rather than to changes of the geometry or spin-distribution.

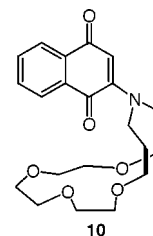
To get insight into the association properties of the crownphanes we chose $7^{\bullet-}$ as a representative example and calculated three different structures of the ion pair $7^{\bullet-}/\text{Li}^+$ (using MNDO, see Table 3). In the first case Li^+ was placed symmetrically above the two phenyl rings carrying the crown ether moiety (A), in the second case above the two other 1,2-diphenyl groups (B), and in the third case above the central double bond (C, Figure 11). We then performed single-point calculations of the Fermi contacts with the B3LYP functional. Whereas the positioning of the counterion at the benzene rings causes a marked redistribution of spin and charge to the positions next to the Li^+ cation, a spin distribution which is comparable to that found on the hyperfine time scale of the ESR experiment emerges when the cation resides at the central (formal) double bond (structure C).

General Conclusions

According to our results, the radical anions and the radical cations of parent **1** and phane derivatives **4–8** have a rather similar structure. The central ethenic bond is twisted by ca. 35° , and the phenyl groups tend to adopt a conformation in which they achieve a more coplanar arrangement than in the neutral stage (enhancement of electron delocalization). This is corroborated by the good correlation between the calculated (UB3LYP/6-31G ** /AM1 or UB3LYP/6-31G ** /UHF/3-21G *) a_{H} and the shapes of the frontier orbitals. Moreover, the experimental data underline the validity of the pairing principle. The rotation of the phenyl groups is restricted, mirrored by the lack of the pairwise equivalence of the ortho and meta protons. Particularly, it was reported that crystallization of the tetraphenylethene radical anion had failed; how-

ever, the X-ray structure determination of the dianion $1^{2-}/2 \text{Na}^+$ reveals a twist angle between the two diphenylmethylene moieties of 56° with the Na^+ counterions above the central (formal) $\text{C}=\text{C}$ bond.⁵² This arrangement is in line with the ion-pair geometry stated for the monoanions.

Radical anions in which a crown-ether moiety is attached to a π system have been described. It was shown that the crown ether may well serve as a ligand to metal cations.^{53–57} In these systems, like **10**, an oxygen



atom carrying a partial negative charge serves as an additional ligand to the metal cation which then is also embedded in the crown-ether moiety. Such an arrangement is not possible in thephanes **4–8**. The negative charge is exclusively delocalized in the tetraphenylethene π system, and the phenyl rings are oriented in such a way that a simultaneous interaction of the crown ether, the π system as the ligands, and the alkali metal atom is not possible. We conclude that the Coulombic attraction between the negatively charged π system and the metal cation is too strong to be matched by the interaction between the crown ether and the cation.

The solution structures of the radical cations closely match the geometry recently established by X-ray diffraction analysis of crystalline tetraanisylethene⁵⁸ where the ethenic bond is twisted by 30.5° and phenyl-ring torsion amounts to 33° (cf. Figure 10). For the radical cations no specific association with counterions could be established by our experimental techniques; however, it is conceivable that metal cations such as Tl^{3+} can be embedded inside the crown ether moiety which is remote from the positively charged π system.

Acknowledgment. We thank the Volkswagen Foundation for financial support and Prof. C. Bolm (Aachen, Germany) for his encouragement. F.B. is indebted to Prof. B. Giese (Basel) for his support.

JO9809200

(52) Bock, H.; Ruppert, K.; Näther, C.; Havlas, Z.; Herrmann, H.-F.; Arad, C.; Göbel, I.; John, A.; Meuret, J.; Nick, S.; Rauschenbach, A.; Seitz, W.; Vaupel, T.; Solouki, B. *Angew. Chem., Int. Ed. Engl.* **1992**, *31*, 550.

(53) Hashimoto, K.; Togo, H.; Morihashi, K.; Yokoyama, Y.; Kikuchi, O. *Bull. Chem. Soc. Jpn.* **1991**, *64*, 3245.

(54) Tajima, K.; Miyoshi, M.; Furutani, M.; Fujimura, Y.; Mukai, K.; Ishizu, K. *Bull. Chem. Soc. Jpn.* **1989**, *62*, 2061.

(55) Bock, H.; Hauck, T.; Naether, C.; Havlas, Z. *Angew. Chem., Int. Ed. Engl.* **1997**, *36*, 638.

(56) Bock, H.; Hierholzer, B.; Voegtler, F.; Hollmann, G. *Angew. Chem.* **1984**, *96*, 74.

(57) Bock, H.; Herrmann, H. F. *J. Am. Chem. Soc.* **1989**, *111*, 7622.

(58) Rathore, R.; Lindeman, S. V.; Kumar, A. S.; Kochi, J. K. *J. Am. Chem. Soc.* **1998**, *120*, 6931.